Published in final edited form as:
Crit Care Med. 2014 July ; 42(7): e491–e500. doi:10.1097/CCM.0000000000000346.

Effect of Local Tidal Lung Strain on Inflammation in Normal and Lipopolysaccharide-Exposed Sheep

Tyler J. Wellman, PhD[1,2], **Tilo Winkler, PhD**[2], **Eduardo L.V. Costa, MD, PhD**[2], **Guido Musch, MD**[2], **R. Scott Harris, MD**[3], **Hui Zheng, PhD**[4], **Jose G. Venegas, PhD**[2], and **Marcos F. Vidal Melo, MD, PhD**[2]

[1]Department of Biomedical Engineering, Boston University, Boston, Massachusetts

[2]Department of Anesthesia, Critical Care and Pain Medicine, Massachusetts General Hospital and Harvard Medical School, Boston, Massachusetts

[3]Pulmonary and Critical Care Unit, Massachusetts General Hospital and Harvard Medical School, Boston, Massachusetts

[4]Biostatistics Center, Massachusetts General Hospital and Harvard Medical School, Boston, Massachusetts

Abstract

Objective—Regional tidal lung strain may trigger local inflammation during mechanical ventilation, particularly when additional inflammatory stimuli are present. However, it is unclear whether inflammation develops proportionally to tidal strain or only above a threshold. We aimed to: (1) assess the relationship between regional tidal strain and local inflammation in vivo during the early stages of lung injury in lungs with regional aeration heterogeneity comparable to that of humans; and (2) determine how this strain-inflammation relationship is affected by endotoxemia.

Design—Interventional animal study.

Setting—Experimental laboratory and positron emission tomography (PET) facility.

Subjects—Eighteen 2–4-month-old sheep.

Interventions—Three groups of sheep (n=6) were mechanically ventilated to the same plateau pressure (30–32 cmH_2O) with High-Strain (V_T=18.2±6.5 ml/kg, PEEP=0), High-Strain plus intravenous lipopolysaccharide (LPS) (V_T=18.4±4.2 ml/kg, PEEP=0), or Low-Strain plus LPS (V_T=8.1±0.2 ml/kg, PEEP=17±3 cmH_2O). At baseline, we acquired respiratory-gated PET scans

Contact Information: Marcos F. Vidal Melo, MD, PhD, Department of Anesthesia, Critical Care, and Pain Medicine, Massachusetts General Hospital and Harvard Medical School, 55 Fruit Street, Boston, MA 02114, USA, mvidalmelo@partners.org.

Institution: This study was performed in the Department of Anesthesia, Critical Care and Pain Medicine, Massachusetts General Hospital and Harvard Medical School, Boston, MA, USA

of inhaled ^{13}NN to measure tidal strain from end-expiratory and end-inspiratory images in six regions of interest (ROIs). After 3 hours of mechanical ventilation, dynamic [^{18}F]fluoro-2-deoxy-D-glucose (^{18}F-FDG) scans were acquired to quantify metabolic activation, indicating local neutrophilic inflammation, in the same ROIs.

Measurements and Main Results—Baseline regional tidal strain had a significant effect on ^{18}F-FDG net uptake rate K_i in High-Strain LPS (p=0.036) and on phosphorylation rate k_3 in High-Strain (p=0.027) and High-Strain LPS (p=0.004). LPS exposure increased the k_3-tidal strain slope 3-fold (p=0.009), without significant lung edema. The Low-Strain LPS group showed lower baseline regional tidal strain (0.33±0.17) than High-Strain (1.21±0.62; p<0.001) or High-Strain LPS (1.26±0.44; p<0.001), and lower k_3 (p<0.001) and K_i (p<0.05) than High-Strain LPS.

Conclusions—Local inflammation develops proportionally to regional tidal strain during early lung injury. The regional inflammatory effect of strain is greatly amplified by intravenous LPS. Tidal strain enhances local ^{18}F-FDG uptake primarily by increasing the rate of intracellular ^{18}F-FDG phosphorylation.

Keywords

Ventilator-Induced Lung Injury; Positron Emission Tomography; Lung Inflammation; Mechanical Ventilation; Lung Strain; Endotoxemia

INTRODUCTION

Ventilator-induced lung injury (VILI) is thought to result from excessive deformation of the lungs during mechanical ventilation (1, 2). This deformation can be described by volumetric strain, defined as the change in lung volume relative to an initial lung volume (2). Protti et al. recently reported a critical threshold of whole-lung strain, corresponding to tidal volumes (V_T) >20 ml/kg, above which ventilator-induced lung edema ultimately develops in normal pigs (3). However, VILI has been shown to develop at significantly lower V_T in patients (4–7) and animals (8, 9). This discrepancy may be explained by at least two factors. First, even presumably safe tidal volumes may produce excessive local strains as a result of strain heterogeneity in supine patients (10) and large animals (11–15). Second, lung sensitivity to strain may increase in the presence of additional inflammatory stimuli, such as lipopolysaccharide (LPS) (16, 17).

Lung inflammation is a key early process in VILI that may precede and contribute to the development of edema. Bellani et al. indicated that pulmonary [^{18}F]fluoro-2-deoxy-D-glucose (^{18}F-FDG) uptake, a well-established marker of neutrophilic inflammation in lung injury (18–22), is linearly related to tidal gas volume changes in normally aerated regions of acute lung injury (ALI) patients mechanical ventilated for 9±7 days (23). However, because they studied the later stages of injury and did not measure tidal strain (24), the role of regional tidal strain in the early development of inflammation remains unclear.

We recently developed a respiratory-gated Positron Emission Tomography (PET) technique to measure regional tidal strain during mechanical ventilation (13), and advanced methods to quantify regional pulmonary inflammation from ^{18}F-FDG kinetics (25, 26). In the present study, we leverage these PET techniques to investigate the following hypotheses in

mechanically ventilated, heterogeneously aerated sheep lungs: (a) regional lung inflammation, assessed from ^{18}F-FDG kinetics, develops in proportion to regional tidal lung strain; (b) the effect of tidal strain on regional inflammation is synergistically increased by systemic LPS exposure; and (c) reduction of regional tidal strain is a major determinant of decreased pulmonary inflammation during protective ventilation.

MATERIALS AND METHODS

Animal Preparation

Study protocols were approved by the Subcommittee on Research Animal Care of the Massachusetts General Hospital, and handling of the animals was in accord with National Institutes of Health guidelines. Sheep (21.5±4.9 kg) were fasted overnight and premedicated with intra-muscular ketamine (4 mg/kg) and midazolam (1–2 mg/kg). Following induction of anesthesia with intravenous propofol (2–4 mg/kg), an endotracheal tube was inserted, and a femoral artery and jugular vein were cannulated. General anesthesia was maintained with continuous infusion of propofol and fentanyl titrated to heart rate and blood pressure. Pancuronium was used for muscle paralysis at induction (0.1 mg/kg) and repeated every 90 minutes (0.02–0.04 mg/kg).

Experimental Procedures

We studied three groups of mechanically ventilated sheep (n=6 animals/group). The first group (High-Strain) aimed to produce high regional tidal strain while avoiding excessive plateau pressure (P_{PLAT}) by using zero positive end-expiratory pressure (PEEP) and continuously adjusting V_T to maintain P_{PLAT} within 30–32 cmH_2O (baseline V_T=18.2±6.5 mL/kg). The second group (High-Strain LPS) combined the same protocol (baseline V_T=18.4±4.2 mL/kg, PEEP=0) with continuous intravenous LPS infusion (10 ng/kg/min, *Escherichia coli* O55:B5, List Biologic Laboratories Inc., Campbell, CA) for the duration of ventilation (3.1±0.8 h), beginning after baseline image acquisition. The third group (Low-Strain LPS) received the same LPS dose and protective ventilation (27), with V_T=8 mL/kg and PEEP continuously adjusted to maintain P_{PLAT}=30–32 cmH_2O (baseline PEEP=17.1±3.4 cmH_2O). This protocol aimed to reduce the tidal (i.e. dynamic) component of lung strain, while maintaining peak strain similar to the other groups.

In each animal, a recruitment maneuver (40 seconds at airway pressure = 35 cmH_2O) was performed at baseline to standardize lung volume history. Additional ventilatory settings were: inspired O_2 fraction (F_IO_2) initially at 0.3 and adjusted to achieve an arterial O_2 saturation >0.88, inspiratory-to-expiratory time ratio I:E=1:2, and respiratory rate RR=18 breaths/minute or higher to maintain the arterial carbon dioxide pressure (P_aCO_2) between 32 and 45 mmHg. A variable dead space was added to the breathing circuit if P_aCO_2 was <32 mmHg with RR=18 breaths/minute.

PET Imaging

Sheep were positioned supine in the PET camera (Scanditronix PC4096, GE Healthcare, Milwaukee, WI), with the most caudal slice of the 9.7 cm field-of-view adjacent to the

diaphragmatic dome. The following scans were acquired after 10 minutes (baseline) or 3.1±0.8 hours of mechanical ventilation (end):

1. Transmission scans (baseline, end): obtained during 10 minutes of continuous breathing to correct emission scans for tissue attenuation and measure lung density. These scans were processed to construct images of average fractional gas content at baseline ($F_{GAS, BL}$) and end ($F_{GAS, END}$) (13).
2. Respiratory-gated ^{13}NN emission scans (baseline, end): acquired to measure regional tidal strain from regional aeration at end-expiration and end-inspiration (13). Briefly, ^{13}NN gas was added to a rebreathing system and equilibrated with the lungs for 6–10 minutes (gas activity~300 kBq/mL). Respiratory-gated imaging was used to track the dynamic changes in pulmonary ^{13}NN concentration during continuous mechanical ventilation. Over a 5-minute acquisition period, images of regional ^{13}NN activity were collected into six bins of equal duration, representing six distinct phases of the respiratory cycle (i.e., two bins during inspiration and four during expiration).
3. ^{18}F-FDG emission scans (end): acquired to assess local metabolic activation (18). ^{18}F-FDG (~200 MBq) was infused over 60 s through a jugular catheter. Simultaneously, a dynamic PET scan was started, consisting of 37 sequential frames (9×10 s, 4×15 s, 1×30 s, 7×60 s, 15×120 s, 1×300 s).

PET images were reconstructed with voxel size of 2×2×6.5 mm using a convolution backprojection algorithm. Images were decay corrected to time zero and filtered in-plane with a circular moving average filter of diameter 12 mm and along the z-axis with a 2-point moving average filter. Each frame yielded a 128×128×14 matrix with effective volumetric resolution of 1.66 cm^3.

Definition of Lung Fields for Analysis

Volumetric masks of lung fields were delineated at both time points (baseline, end) for end-expiration (EE), end-inspiration (EI), and mean lung volume by: (a) including all voxels with F_{GAS}>0.5; (b) adding perfused but poorly-aerated lung regions viewed in the end-apnea frames of the ^{13}NN infusion scan; and (c) manually excluding the trachea, two main bronchi, and major blood vessels. Six regions-of-interest (ROIs) were defined for each animal by dividing the lung field in half along the cephalo-caudal axis, and further dividing each half along the ventral-dorsal axis into three sub-regions of equal height (Figure 1A).

Image Analysis

End-expiratory and end-inspiratory images of equilibrated ^{13}NN were normalized by the ^{13}NN specific activity to obtain images of fractional gas content at end-expiration (F_{EE}) and end-inspiration (F_{EI}) (13). In each ROI, tidal specific volume change (sVol, defined as the change in gas volume during inspiration divided by end-expiratory gas volume) was computed from average F_{EE} and F_{EI}, according to Fuld et al. (11):

$$sVol = \frac{F_{EI} - F_{EE}}{F_{EE}(1 - F_{EI})}$$

In corresponding ROIs in the ^{18}F-FDG images, the three-compartment Sokoloff model (28) was fit to ^{18}F-FDG kinetics using iterative optimization. The ^{18}F-FDG concentration within a blood pool ROI drawn over the right heart was used as an input function for the model after calibration with manual blood samples (29). For each ROI, we obtained three parameters describing ^{18}F-FDG kinetics: the fractional distribution volume of ^{18}F-FDG in tissue (F_e), the rate of ^{18}F-FDG phosphorylation (k_3), and the net uptake rate (K_i), where $K_i=F_e \cdot k_3$.

Statistical Analysis

Data are presented as mean ± standard deviation unless otherwise noted, and significance was set at $p<0.05$. Global variables were compared between groups using one-way ANOVA with Tukey-Kramer post-hoc tests for normally distributed data, or Kruskal-Wallis with Bonferroni-corrected Mann-Whitney tests otherwise. All regional measurements, including sVol, F_{EE}, F_{EI}, K_i, F_e, and k_3, were compared between groups using linear mixed-effects models with group (categorical) as a fixed effect and random intercepts for each animal to account for repeated measurements (i.e., six ROIs per animal). To test for effects of ROI position on sVol, we also modeled sVol with fixed effects for ROI ventral-dorsal and cephalo-caudal positions in each group, and random intercepts and position effects in each animal. To determine effects of sVol on ^{18}F-FDG parameters, we modeled each ^{18}F-FDG parameter (K_i, F_e, and k_3) as an interaction between sVol and group (i.e. allowing different effects of sVol in each group) and included random intercepts and sVol effects for each animal. A heterogeneous covariance structure was used in the K_i, F_e, and k_3 models, to allow for different variances among groups. All analyses were performed using Matlab (R2013b Statistics Toolbox, The Mathworks, Natick, MA).

RESULTS

Global Cardiorespiratory Variables

Consistent with the study design, High-Strain groups received higher V_T and lower levels of PEEP and respiratory rates than the Low-Strain LPS group (Table 1). P_aO_2/F_IO_2 decreased by the end of the study only in the High-Strain LPS group.

Topographic Heterogeneity of Tidal Strain

At baseline, the High-Strain groups showed large, heterogeneous changes in aeration between end-expiration and end-inspiration (Figure 2, Supplemental Digital Content 1). In contrast, animals in the Low-Strain LPS group showed smaller and more homogeneously distributed tidal changes in aeration. There was a significant gravitational dependence of sVol, with highest values in dependent regions, in both the High-Strain ($p<0.001$) and High-Strain LPS groups ($p=0.004$), but not in the Low-Strain LPS group (Figure 1B). No dependence of sVol on ROI cephalo-caudal position was detected in any group.

The magnitude of regional sVol was different among the groups at baseline, as expected from the applied ventilator settings. Both High-Strain groups presented significantly higher sVol than the Low-Strain LPS group (Table 2, Figure 1B). Of note, in the High-Strain groups, a considerable fraction of ROIs presented sVol>1.5 (28% of all non-LPS ROIs, 17%

for LPS), with some regions even showing sVol>2 (8% for both), despite global sVol values (computed from whole-lung average F_{EE} and F_{EI}) being close to 1 (Table 2). Measurements of sVol at the end of the experiments reflected similar distributions to those at baseline (Table 2, Figure 1C). No systematic changes in sVol over time were observed in any of the groups. Strong correlations were found between sVol at the end and baseline sVol for measurements from all groups ($sVol_{end}=0.76 \cdot sVol_{baseline}+0.15$, r=0.76, p<0.001), indicating stable topographic distributions of sVol over time.

Relation of Regional Metabolic Activation with Tidal Strain

Regional ^{18}F-FDG net uptake rate K_i, volume of distribution F_e, and rate of phosphorylation k_3 showed significant gravitational dependence (Supplemental Digital Content 2), with highest values in dependent regions (Figure 2). Applying the mixed-effects model to measurements in ROIs, K_i showed a significant linear association with sVol in the High-Strain LPS group (p=0.036), but not in the High-Strain or Low-Strain LPS groups (Figure 3A). The components of K_i ($K_i=F_e \cdot k_3$) were differently associated with regional strain. Whereas the ^{18}F-FDG volume of distribution F_e was not associated with sVol in any of the groups (Figure 3B), the ^{18}F-FDG rate of phosphorylation k_3 was associated with sVol in the High-Strain (p=0.027) and High-Strain LPS groups (p=0.004) (Figure 3C) but not in the Low-Strain LPS group (Figure 3D). The High-Strain LPS group showed higher values of k_3 (p<0.001) than the Low-Strain LPS group. These findings imply that the increase in K_i with increasing sVol following LPS exposure occurred predominantly through a higher k_3, indicating enhanced intra-cellular phosphorylation of ^{18}F-FDG in regions with higher tidal strain.

Effect of LPS on the Relationship between Tidal Strain and Metabolic Activation

By exposing the lungs to LPS during High-Strain ventilation, the magnitude of the effect of sVol on k_3 increased by a factor of 3.3 (2.14×10^{-2} vs. 0.65×10^{-2} min^{-1}, p=0.009, Figure 3C). Thus, the lung metabolic response to tidal strain was enhanced by more than a factor of 3 in the presence of LPS. This increase in the k_3 vs. sVol slope with LPS exposure was clearly evident by examining individual animal regressions [0]in the mixed-effects model (Supplemental Digital Content 3). In addition to these differences in slope, intercepts of the mixed-effects model of k_3 tended to be higher in LPS groups (High-Strain =3.90×10^{-2} min^{-1}, Low-Strain =3.86×10^{-2} min^{-1}) than in the High-Strain group (2.45×10^{-2} min^{-1}, p=0.108 vs. High-Stain LPS, p=0.022 vs. Low-Strain LPS, Figure 3C). These results suggest that LPS has both an independent effect on metabolic activation, as well as an important interaction with tidal strain that further increases metabolic activation.

Data from the Low-Strain LPS group were highly concentrated in the k_3–sVol plot (Figure 3D), highlighting the homogeneity of those variables in this group. Importantly, those points fell along the mixed-model regression line defined by the High-Strain LPS group. To show this quantitatively, the data were grouped according to LPS exposure and reanalyzed with the mixed-effects model (i.e., Low-Strain and High-Strain LPS groups combined). In this model, parameters of the combined LPS group were not significantly different from those of the High-Strain LPS alone (Figure 3D), in terms of slope (1.96×10^{-2} [all LPS] vs. 2.14×10^{-2} [High-Strain LPS only] min^{-1}, p=0.79) or intercept (3.58×10^{-2} vs. 3.90×10^{-2}

min^{-1}, p=0.60). Given that data from all LPS-exposed animals followed the same global trend (dotted line, Figure 3D), the reduction in metabolic activation with protective (i.e., Low-Strain) ventilation presumably occurred through the reduction of sVol, shifting lung regions downward along that regression line.

The maximum regional k_3 was highest in the High-Strain LPS group (Figure 4). Among LPS-exposed animals, Low-Strain ventilation reduced the maximum k_3 by 43% ($p<0.05$). Comparing High-Strain groups, there was a trend toward higher minimum k_3 with LPS ($p<0.10$), supporting the presence of a small independent effect of LPS on metabolic activation even in regions of lowest tidal strain.

Additional Variables Influencing Regional Inflammation

In addition to tidal strain, we also studied the associations of k_3 with other variables potentially influencing inflammation: regional tidal recruitment, perfusion, average lung inflation level (F_{GAS}), hyper-inflation, consolidated atelectasis, and intra-regional heterogeneity of tidal strain (Supplemental Digital Content 1). Using the same mixed-effects model used to study the association of sVol with k_3, we found no associations of perfusion or hyper-inflation with k_3. Average F_{GAS} was inversely associated with k_3 in all groups. In the High-Strain LPS group but not in the High-Strain group, k_3 was associated with tidal recruitment of voxels with $F_{GAS}<0.1$ ($p=0.019$) and $0.1<F_{GAS}<0.3$ ($p<0.001$; Figure 5), as well as with intra-regional heterogeneity of specific ventilation ($p=0.002$), measured from ^{13}NN washout (30). Among all studied independent variables, sVol was the most strongly associated with regional k_3 in lungs with and without LPS exposure (Supplemental Digital Content 1).

Histological Injury

Regional tissue injury was mild in all groups (Supplemental Digital Content 4). LPS exposure significantly increased tissue neutrophil counts in both ventral and dorsal regions, with similar neutrophil counts between LPS groups. No interstitial or alveolar edema was observed in any group.

DISCUSSION

Using sheep models of early acute lung injury, we found that: (a) mechanical ventilation in the supine position with zero PEEP and high tidal volumes results in topographically heterogenenous local tidal strain, with highest values in dependent regions; (b) in both normal and LPS-exposed lungs ventilated with high tidal volumes, ^{18}F-FDG phosphorylation rate k_3 is significantly associated with regional tidal strain; (c) exposure to LPS substantially increases the slope of the k_3 vs. sVol regression, indicating local synergistic interaction between tidal strain and LPS; and (d) use of low tidal volumes and high PEEP decreases the magnitude of regional tidal strain and produces a corresponding reduction in k_3, supporting a direct effect of tidal strain on regional metabolic activation.

We found significant topographic heterogeneity of tidal strain in the High-Strain groups. Of note, a substantial fraction of lung regions presented sVol>1.5, despite global values being close to 1, reinforcing that high levels of regional strain may be present even when global

strain is within a presumably safe range (11–15, 31). Although we used relatively large V_T to achieve those high strains, ARDS lungs may exhibit similar levels of strain at much lower V_T. In fact, Chiumello et al. found global strains in the range of 1–1.5 in patients ventilated with V_T between 6–12 ml/kg and PEEP = 5 cmH_2O (32). Considering the substantial heterogeneity of strain and compliance observed in ARDS models (14, 33), it is plausible that local strains as high as 2 could exist in patients with global strains >1.

Tidal strain appeared to have a direct effect on the regional ^{18}F-FDG net uptake rate K_i in lungs with LPS exposure. We and others have established that K_i is a sensitive marker of neutrophilic inflammation in humans (34, 35) and animal models of lung injury (19–21). Since K_i is the product of k_3 and F_e, we further examined the dependence of these K_i components on tidal strain. We found that k_3 had the strongest associations with sVol, both with and without LPS exposure, while F_e showed no associations with sVol. In contrast to K_i and F_e, which are expected to be linearly related to local tissue density, k_3 should not depend directly on tissue density, as it represents the average rate of intracellular ^{18}F-FDG phosphorylation within the tissue compartment of a region-of-interest (28). Indeed, given that $K_i=F_e \bullet k_3$, if F_e is linearly related to tissue density (as supported by our data in Supplemental Digital Content 2), k_3 must be independent from it in order to confer the linear dependence of K_i on tissue density. Thus, k_3 is expected to depend only on the specific metabolic state of the cells present in the tissue, providing an index of cellular metabolic activity independent of tissue density. In the High-Strain group, increased k_3 in response to tidal stretching may have resulted from normal physiologic responses to stretch such as deformation-induced lipid trafficking (36) or cytoskeletal reorganization (37). Given the high neutrophil counts observed after LPS exposure, the increased metabolic activation with strain in LPS animals more likely reflects the triggering of inflammatory processes, with increased number and activation of neutrophils as well as contributions from other cells (38). Interestingly, while neutrophil counts were similar between the LPS groups, metabolic activation was significantly greater with High-Strain than with Low-Strain ventilation, suggesting that tidal strain primarily affected the activation of sequestered neutrophils, rather than causing recruitment of additional neutrophils.

Intravenous LPS remarkably amplified the effect of tidal strain on metabolic activation, increasing the slope of the k_3–sVol regression by more than a factor of 3. Thus, the increase in metabolic activation caused by a moderate LPS dose was larger in regions of higher tidal strain, implying the presence of local synergy between tidal strain and LPS. While synergy between stretch and LPS in producing cytokine release has been documented in isolated epithelial cells (39), macrophages (40), and small animal models (16, 17), our findings demonstrate the relevance of *regional* interactions between strain and other inflammatory stimuli in large, heterogeneous lungs. Such interactions could play an important role in generating the marked topographic heterogeneity of inflammation observed in ARDS patients (41). Additionally, increased sensitivity of the lungs to tidal strain when additional inflammatory stimuli are present may help to reconcile the findings of Protti et al., where injury did not occur until V_T>20 ml/kg (3), with evidence of VILI in patients ventilated with much lower V_T (5, 42–44).

The absence of histological lung edema in all groups, despite significant neutrophilic inflammation in the LPS groups, suggests that the inflammatory response to tidal strain may either precede the formation of edema, or occur at lower values of strain, below the threshold for edema if such exists. Accordingly, our findings suggest that metabolic changes may be more sensitive than measurements of edema for detection of early processes in the development of lung injury. Importantly, the observed association between regional lung strain and inflammation occurred over a range of strain values lower than those whole-lung strains previously observed to cause edema (3). Thus, even if strains applied in routine mechanical ventilation are not large enough to ultimately produce edema, such strains could still trigger early inflammation, potentially with clinically relevant consequences.

Mechanical and physiologic factors other than tidal strain may have provoked inflammation in our studies. In the High-Strain LPS group, we found associations of k_3 with tidal recruitment and ventilation heterogeneity (Supplemental Digital Content 1), though these were not as strong as the association with tidal strain. Nonetheless, it is possible that low-volume injury mechanisms may have contributed to the genesis of inflammation in this group. Indeed, high interfacial stresses that occur during tidal recruitment can injure epithelial cell plasma membranes (45, 46). In normal lungs (e.g., High-Strain group), healthy surfactant function may prevent or delay injury by these mechanisms. However, LPS-dependent surfactant dysfunction can produce higher surface tensions (47), with consequent increase in the risk of cell injury. Such effects of LPS could be partly responsible for the observed association between inflammation and tidal recruitment in the High-Strain LPS animals. However, our data point to tidal strain as a more important determinant of early regional inflammation in the studied normal and LPS-exposed lungs.

Our finding that average lung inflation (i.e., F_{GAS}) was negatively associated with metabolic activation (Supplemental Digital Content 1) suggests that inflammation was not provoked by high static (i.e., continuously applied) strain, but by the dynamic component of strain induced by tidal inflation. This result is in line with recent findings of dynamic strain as a more important determinant of whole-lung edema and inflammation than static strain (3). We expand on those findings by showing that this predominant sensitivity of the lungs to dynamic strain applies to the early regional development of inflammation, before any histologic measures of tissue injury or edema are detectable.

Methodological limitations to our study include: (a) Our measurements of sVol could be affected by tidal recruitment. PET estimates of recruitment were associated with k_3, yet less so than tidal strain and only in the High-Strain LPS group (Supplemental Digital Content 1). Higher resolution CT techniques may be required to further study the respective roles of recruitment and tidal strain. (b) We computed strain using end-expiratory gas volume in the denominator as done previously (48), though others have used functional residual capacity (49). While the definition of lung “resting volume” remains arbitrary (1) and will affect the computation of strain (2), our choice was consistent with the goal of quantifying the dynamic component of strain in the studied conditions. (c) Registration errors between end-expiration and end-inspiration could produce error in sVol measurements. We mitigated this by studying large ROIs (13) and computing sVol from average regional F_{EE} and F_{EI}, which are relatively insensitive to registration errors (11, 13); (d) Regional metabolic activation

was used as a surrogate for inflammation. Although we did not measure tissue markers of inflammation (e.g. cytokines), ^{18}F-FDG uptake in itself is an established marker of neutrophilic inflammation in acutely injured lungs (18–22, 50).

CONCLUSIONS

During mechanical ventilation of supine lungs similar in size to human lungs, high regional lung strains may be present even when global lung strain is within acceptable limits. Regional lung metabolic activation, reflecting the development of local inflammation, shows a positive linear relation with tidal strain, and this dependence is substantially amplified by moderate LPS exposure even when lung edema is not apparent. Such localized metabolic activation is prevented by reducing and homogenizing regional tidal strain with high PEEP and low V_T.

Supplementary Material

Refer to Web version on PubMed Central for supplementary material.

Acknowledgments

Financial Support: Supported by grants R01-HL086827 and R01-HL121228 from the National Heart, Lung, and Blood Institute. G. Musch was supported in part by grant R01-HL094639.

We would like to thank the cyclotron staff for isotope preparation and Steven B. Weise for expert technical assistance in image acquisition and reconstruction. We also thank Dr. Bela Suki for his insight and criticism of the manuscript.

References

1. Plataki M, Hubmayr RD. The physical basis of ventilator-induced lung injury. Expert Rev Respir Med. 2010; 4:373–385. [PubMed: 20524920]
2. Gattinoni L, Carlesso E, Caironi P. Stress and strain within the lung. Curr Opin Crit Care. 2012; 18:42–47. [PubMed: 22157254]
3. Protti A, Cressoni M, Santini A, et al. Lung stress and strain during mechanical ventilation: Any safe threshold? Am J Respir Crit Care Med. 2011; 183:1354–1362. [PubMed: 21297069]
4. Gajic O, Dara SI, Mendez JL, et al. Ventilator-associated lung injury in patients without acute lung injury at the onset of mechanical ventilation. Crit Care Med. 2004; 32:1817–1824. [PubMed: 15343007]
5. Acute Respiratory Distress Syndrome Network. Ventilation with lower tidal volumes as compared with traditional tidal volumes for acute lung injury and the acute respiratory distress syndrome. the acute respiratory distress syndrome network. N Engl J Med. 2000; 342:1301–1308. [PubMed: 10793162]
6. Amato MB, Barbas CS, Medeiros DM, et al. Effect of a protective-ventilation strategy on mortality in the acute respiratory distress syndrome. N Engl J Med. 1998; 338:347–354. [PubMed: 9449727]
7. Serpa Neto A, Cardoso SO, Manetta JA, et al. Association between use of lung-protective ventilation with lower tidal volumes and clinical outcomes among patients without acute respiratory distress syndrome: A meta-analysis. JAMA. 2012; 308:1651–1659. [PubMed: 23093163]
8. Gharib SA, Liles WC, Klaff LS, et al. Noninjurious mechanical ventilation activates a proinflammatory transcriptional program in the lung. Physiol Genomics. 2009; 37:239–248. [PubMed: 19276240]

9. Wolthuis EK, Vlaar AP, Choi G, et al. Mechanical ventilation using non-injurious ventilation settings causes lung injury in the absence of pre-existing lung injury in healthy mice. Crit Care. 2009; 13:R1. [PubMed: 19152704]
10. Guerrero T, Sanders K, Noyola-Martinez J, et al. Quantification of regional ventilation from treatment planning CT. Int J Radiat Oncol Biol Phys. 2005; 62:630–634. [PubMed: 15936537]
11. Fuld MK, Easley RB, Saba OI, et al. CT-measured regional specific volume change reflects regional ventilation in supine sheep. J Appl Physiol. 2008; 104:1177–1184. [PubMed: 18258804]
12. Reinhardt JM, Ding K, Cao K, et al. Registration-based estimates of local lung tissue expansion compared to xenon CT measures of specific ventilation. Med Image Anal. 2008; 12:752–763. [PubMed: 18501665]
13. Wellman TJ, Winkler T, Costa EL, et al. Measurement of regional specific lung volume change using respiratory-gated PET of inhaled 13N-nitrogen. J Nucl Med. 2010; 51:646–653. [PubMed: 20237036]
14. Kaczka DW, Cao K, Christensen GE, et al. Analysis of regional mechanics in canine lung injury using forced oscillations and 3D image registration. Annals of Biomedical Engineering. 2011; 39:1112–1124. [PubMed: 21132371]
15. Fernandez-Bustamante A, Easley RB, Fuld M, et al. Regional pulmonary inflammation in an endotoxemic ovine acute lung injury model. Respir Physiol Neurobiol. 2012; 183:149–158. [PubMed: 22728442]
16. Bregeon F, Delpierre S, Chetaille B, et al. Mechanical ventilation affects lung function and cytokine production in an experimental model of endotoxemia. Anesthesiology. 2005; 102:331–339. [PubMed: 15681948]
17. Altemeier WA, Matute-Bello G, Frevert CW, et al. Mechanical ventilation with moderate tidal volumes synergistically increases lung cytokine response to systemic endotoxin. Am J Physiol Lung Cell Mol Physiol. 2004; 287:L533–42. [PubMed: 15145786]
18. Costa EL, Musch G, Winkler T, et al. Mild endotoxemia during mechanical ventilation produces spatially heterogeneous pulmonary neutrophilic inflammation in sheep. Anesthesiology. 2010; 112:658–669. [PubMed: 20179503]
19. Musch G, Venegas JG, Bellani G, et al. Regional gas exchange and cellular metabolic activity in ventilator-induced lung injury. Anesthesiology. 2007; 106:723–735. [PubMed: 17413910]
20. Saha D, Takahashi K, de Prost N, et al. Micro-autoradiographic assessment of cell types contributing to 2-deoxy-2-[(18)F]fluoro-D-: Glucose uptake during ventilator-induced and endotoxemic lung injury. Mol Imaging Biol. 2012
21. Jones HA, Clark RJ, Rhodes CG, et al. In vivo measurement of neutrophil activity in experimental lung inflammation. Am J Respir Crit Care Med. 1994; 149:1635–1639. [PubMed: 7516252]
22. Hartwig W, Carter EA, Jimenez RE, et al. Neutrophil metabolic activity but not neutrophil sequestration reflects the development of pancreatitis-associated lung injury. Crit Care Med. 2002; 30:2075–2082. [PubMed: 12352044]
23. Bellani G, Guerra L, Musch G, et al. Lung regional metabolic activity and gas volume changes induced by tidal ventilation in patients with acute lung injury. Am J Respir Crit Care Med. 2011; 183:1193–1199. [PubMed: 21257791]
24. Bellani G, Pesenti A, Musch G. Regional lung strain and inflammation. American Journal of Respiratory and Critical Care Medicine. 2012; 185:229–230.
25. Schroeder T, Vidal Melo MF, Musch G, et al. Modeling pulmonary kinetics of 2-deoxy-2-[(18)F]fluoro-d-glucose during acute lung injury. Acad Radiol. 2008; 15:763–775. [PubMed: 18486012]
26. Dittrich AS, Winkler T, Wellman T, et al. Modeling (18)F-FDG kinetics during acute lung injury: Experimental data and estimation errors. PLoS One. 2012; 7:e47588. [PubMed: 23118881]
27. Mercat A, Richard JC, Vielle B, et al. Positive end-expiratory pressure setting in adults with acute lung injury and acute respiratory distress syndrome: A randomized controlled trial. JAMA. 2008; 299:646–655. [PubMed: 18270353]
28. Sokoloff L, Reivich M, Kennedy C, et al. The [14C]deoxyglucose method for the measurement of local cerebral glucose utilization: Theory, procedure, and normal values in the conscious and anesthetized albino rat. J Neurochem. 1977; 28:897–916. [PubMed: 864466]

29. Schroeder T, Vidal Melo MF, Musch G, et al. Image-derived input function for assessment of 18F-FDG uptake by the inflamed lung. J Nucl Med. 2007; 48:1889–1896. [PubMed: 17942803]
30. Wellman TJ, Winkler T, Costa EL, et al. Effect of regional lung inflation on ventilation heterogeneity at different length scales during mechanical ventilation of normal sheep lungs. J Appl Physiol. 2012; 113:947–957. [PubMed: 22678958]
31. Valenza F, Guglielmi M, Maffioletti M, et al. Prone position delays the progression of ventilator-induced lung injury in rats: Does lung strain distribution play a role? Crit Care Med. 2005; 33:361–367. [PubMed: 15699840]
32. Chiumello D, Carlesso E, Cadringher P, et al. Lung stress and strain during mechanical ventilation for acute respiratory distress syndrome. Am J Respir Crit Care Med. 2008; 178:346–355. [PubMed: 18451319]
33. Perchiazzi G, Rylander C, Vena A, et al. Lung regional stress and strain as a function of posture and ventilatory mode. J Appl Physiol. 2011; 110:1374–1383. [PubMed: 21393463]
34. Jones HA, Sriskandan S, Peters AM, et al. Dissociation of neutrophil emigration and metabolic activity in lobar pneumonia and bronchiectasis. Eur Respir J. 1997; 10:795–803. [PubMed: 9150315]
35. Chen DL, Rosenbluth DB, Mintun MA, et al. FDG-PET imaging of pulmonary inflammation in healthy volunteers after airway instillation of endotoxin. J Appl Physiol. 2006; 100:1602–1609. [PubMed: 16424067]
36. Vlahakis NE, Schroeder MA, Pagano RE, et al. Deformation-induced lipid trafficking in alveolar epithelial cells. Am J Physiol Lung Cell Mol Physiol. 2001; 280:L938–46. [PubMed: 11290518]
37. Putnam AJ, Schultz K, Mooney DJ. Control of microtubule assembly by extracellular matrix and externally applied strain. Am J Physiol Cell Physiol. 2001; 280:C556–64. [PubMed: 11171575]
38. Saha D, Takahashi K, de Prost N, et al. Micro-autoradiographic assessment of cell types contributing to 2-deoxy-2-[(18)f]fluoro-d-glucose uptake during ventilator-induced and endotoxemic lung injury. Mol Imaging Biol. 2013; 15:19–27. [PubMed: 22752654]
39. Ning QM, Wang XR. Response of alveolar type II epithelial cells to mechanical stretch and lipopolysaccharide. Respiration. 2007; 74:579–585. [PubMed: 17435381]
40. Pugin J, Dunn I, Jolliet P, et al. Activation of human macrophages by mechanical ventilation in vitro. Am J Physiol. 1998; 275:L1040–50. [PubMed: 9843840]
41. Bellani G, Messa C, Guerra L, et al. Lungs of patients with acute respiratory distress syndrome show diffuse inflammation in normally aerated regions: A [18F]-fluoro-2-deoxy-D-glucose PET/CT study. Crit Care Med. 2009; 37:2216–2222. [PubMed: 19487931]
42. Determann RM, Royakkers A, Wolthuis EK, et al. Ventilation with lower tidal volumes as compared with conventional tidal volumes for patients without acute lung injury: A preventive randomized controlled trial. Crit Care. 2010; 14:R1. [PubMed: 20055989]
43. Wolthuis EK, Choi G, Dessing MC, et al. Mechanical ventilation with lower tidal volumes and positive end-expiratory pressure prevents pulmonary inflammation in patients without preexisting lung injury. Anesthesiology. 2008; 108:46–54. [PubMed: 18156881]
44. Pinheiro de Oliveira R, Hetzel MP, dos Anjos Silva M, et al. Mechanical ventilation with high tidal volume induces inflammation in patients without lung disease. Crit Care. 2010; 14:R39. [PubMed: 20236550]
45. Oeckler RA, Hubmayr RD. Cell wounding and repair in ventilator injured lungs. Respir Physiol Neurobiol. 2008; 163:44–53. [PubMed: 18638574]
46. Hussein O, Walters B, Stroetz R, et al. Biophysical determinants of alveolar epithelial plasma membrane wounding associated with mechanical ventilation. Am J Physiol Lung Cell Mol Physiol. 2013; 305:L478–84. [PubMed: 23997173]
47. Kennedy M, Phelps D, Ingenito E. Mechanisms of surfactant dysfunction in early acute lung injury. Exp Lung Res. 1997; 23:171–189. [PubMed: 9184787]
48. Gonzalez-Lopez A, Garcia-Prieto E, Batalla-Solis E, et al. Lung strain and biological response in mechanically ventilated patients. Intensive Care Med. 2012; 38:240–247. [PubMed: 22109653]
49. Caironi P, Cressoni M, Chiumello D, et al. Lung opening and closing during ventilation of acute respiratory distress syndrome. Am J Respir Crit Care Med. 2010; 181:578–586. [PubMed: 19910610]

50. de Prost N, Costa EL, Wellman T, et al. Effects of ventilation strategy on distribution of lung inflammatory cell activity. Crit Care. 2013; 17:R175. [PubMed: 23947920]

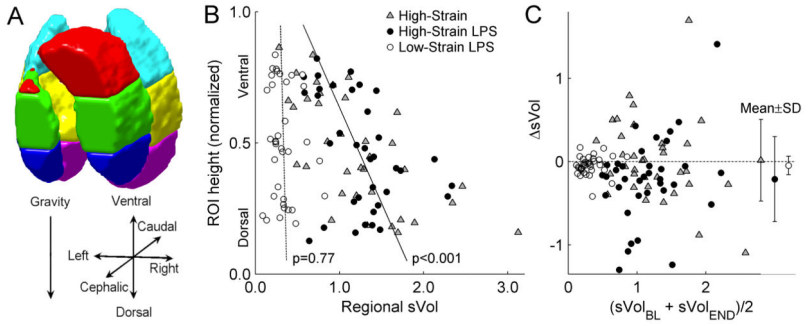

Figure 1.

(A) Configuration of regions-of-interest (ROIs) for sVol computation, (B) distributions of baseline sVol ($sVol_{BL}$) along the gravitational axis, and (C) changes in sVol (ΔsVol) from baseline to the study end ($sVol_{END}$). Use of 6 ROIs in each sheep (A) resulted in a median ROI volume of 89 mL, with distinct ROI positions along the gravitational axis. Mixed-model regression lines in (B) show a significant gravitational dependence of $sVol_{BL}$ in the combined High-Strain (gray triangles) and High-Strain LPS (black circles) groups, but not in the Low-Strain LPS group (white circles). Values of ΔsVol were mostly small (C), with averages (mean±SD) close to zero. No systematic change in sVol was observed in any of the groups.

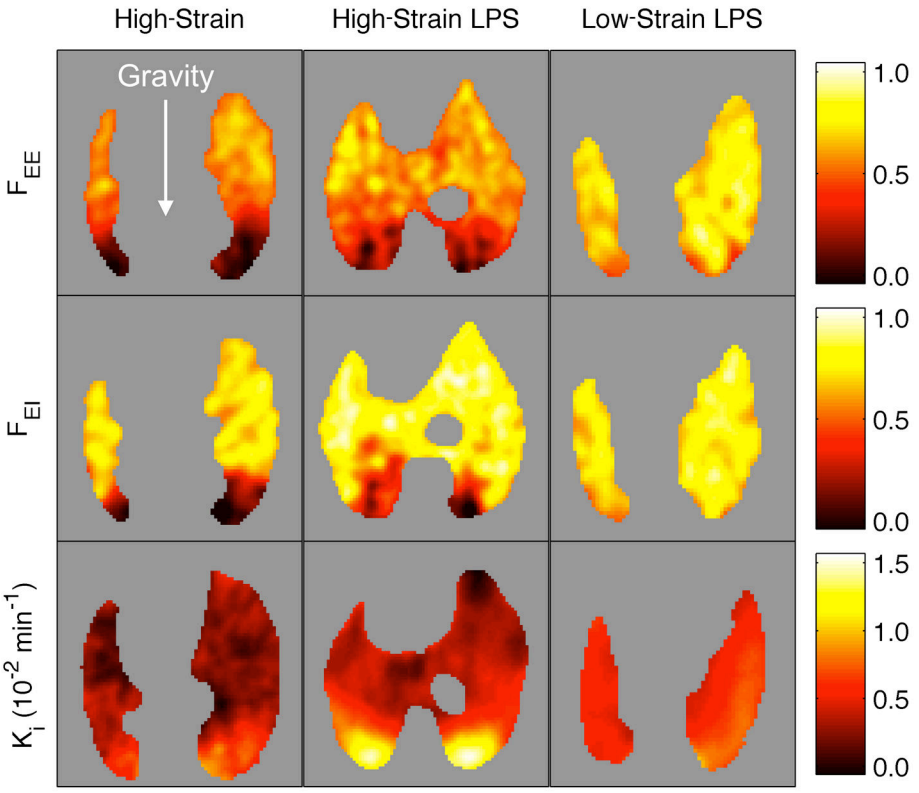

Figure 2.

Images of transverse planes from a representative animal in each group. Fractional gas content at end-expiration (F_{EE}) and end-inspiration (F_{EI}) as well as ^{18}F-FDG net uptake rate (K_i) showed notable heterogeneity along the gravitational axis in both High-Strain groups. With High-Strain ventilation, K_i increased with LPS exposure, particularly in the dependent lung. Concentrated ^{18}F-FDG uptake was not observed with protective ventilation (Low-Strain), where F_{EE} and F_{EI} were more homogeneous and LPS appeared to produce a small global increase in K_i.

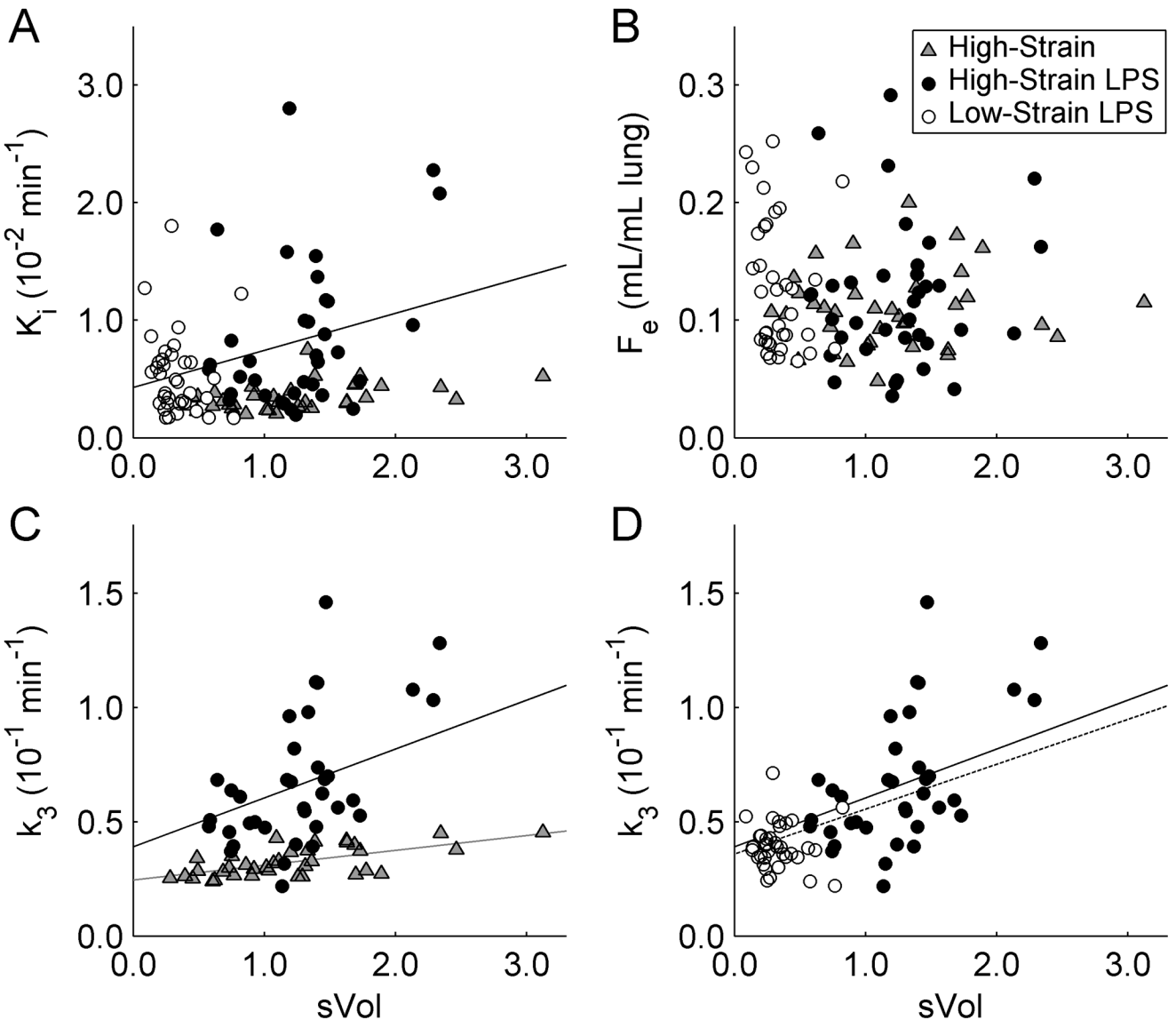

Figure 3.

(A) ^{18}F-FDG net uptake rate K_i, (B) volume of distribution F_e, and (C,D) phosphorylation rate k_3 vs. regional sVol for all ROIs of all animals in the High-Strain group (gray triangles), High-Strain LPS group (black circles), and Low-Strain LPS group (white circles). Regression lines in (A,C) show significant effects of sVol in the High-Strain (gray line) and High-Strain LPS (black line) groups, determined with the mixed-effects models of K_i and k_3. No significant effects of sVol were found in the Low-Strain LPS group. (C) Comparing the High-Strain groups, the slope of k_3 vs. sVol was 3.3 times higher ($p=0.009$) and the intercept was 60% higher ($p=0.108$) with LPS exposure. (D) Comparing the LPS groups, the Low-Strain protocol led to lower values of sVol ($p<0.001$) and k_3 ($p<0.001$), which fell along the same k_3–sVol relationship defined by the High-Strain LPS group. When the mixed-effects model was fit to all LPS animals together (dotted line), the regression line was

not significantly different from that of High-Strain LPS alone (solid line), implying a similar dependence of k_3 on sVol in all LPS animals.

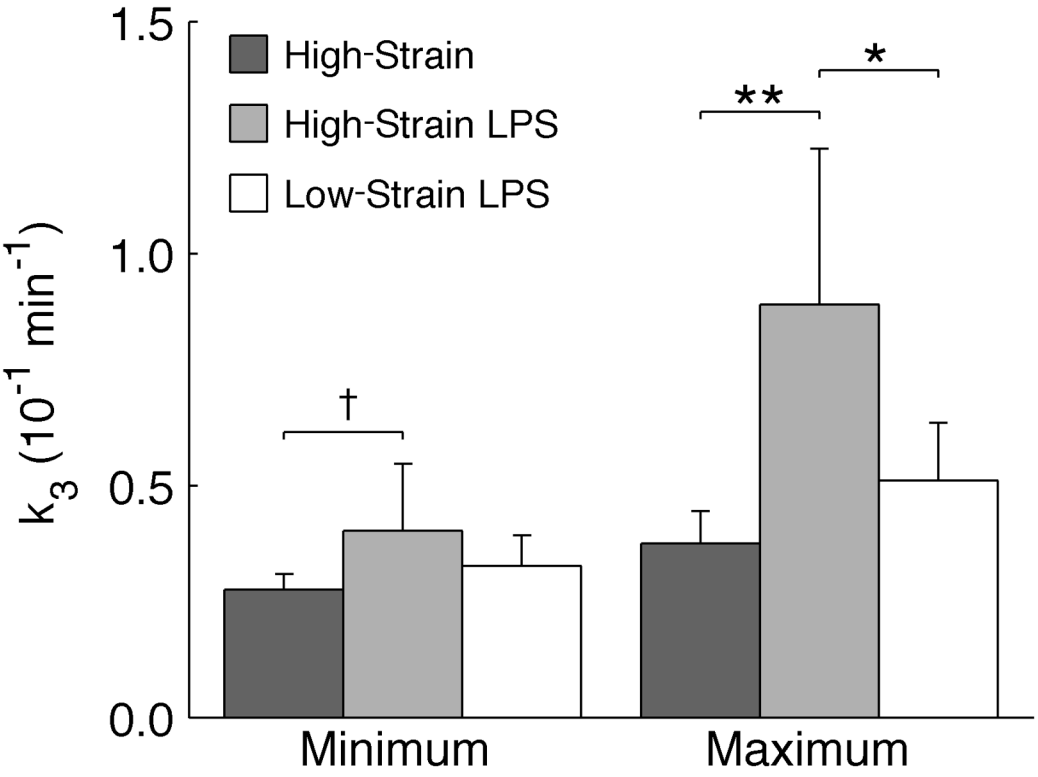

Figure 4.

Minimum and maximum regional k_3 in each group. Comparing High-Strain groups, LPS appeared to have a small effect on minimum k_3, and significantly increased maximum k_3. Comparing LPS groups, the Low-Strain LPS protocol greatly reduced the maximum k_3 in relation to High-Strain LPS, though minimum values of k_3 were similar. $^{\dagger}p<0.10$, $*p<0.05$, $**p<0.01$.

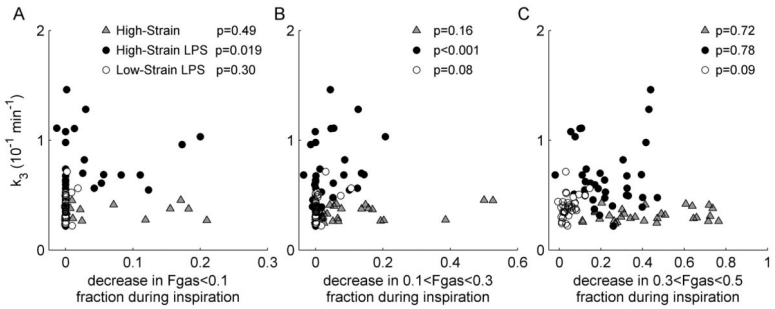

Figure 5.

Relation between regional ^{18}F-FDG phosphorylation rate k_3 and estimates of tidal recruitment of distinct aeration compartments, based on decrease in the fractions of voxels in those compartments during inspiration. Significance of the effect of each predictor variable, derived with the mixed-effects models, is shown for each group.

Table 1

Weight and Cardiorespiratory Variables

	High-Strain (n=6)		High-Strain LPS (n=6)		Low-Strain LPS (n=6)	
	Baseline	**End**	**Baseline**	**End**	**Baseline**	**End**
Weight, kg	20 (18–21)		23 (21–24)		20 (19–21)	
V_T, mL·kg^{-1}	18.2 (17.0–23.5)^{b}	20.0 (13.9–24.3)^{b}	18.8 (15.9–21.5)^{b}	13.8 (11.5–18.7)^{b,e}	8.1 (8.0–8.3)	8.0 (7.9–8.1)
PEEP, cmH_2O	0 ± 0^{b}	0 ± 0 ^{b}	0 ± 0 ^{b}	0 ± 0^{b}	17 ± 3	17 ± 2
RR, bpm	19 ± 1^{b}	19 ± 3	19 ± 2^{b}	21 ± 3	25 ± 2	26 ± 2
F_IO_2	0.3 (0.3–0.3)	0.35 (0.3–0.4)	0.3 (0.3–0.35)	0.35 (0.3–0.6)	0.3 (0.3–0.4)	0.3 (0.3–0.4)
CO, L·min^{-1}	5.9 ± 1.3 ^{b}	6.3 ± 1.2^{b}	4.4 ± 1.1	4.4 ± 0.7 ^{b,c}	3.3 ± 0.7	3.2 ± 0.5
MAP, mmHg	74 ± 14	81c 13	92 ± 12	78 ± 13 ^{f}	87 ± 13	81 ± 13
MPAP, mmHg	14 ± 8	15 ± 9 ^{b}	16 ± 9	21 ± 5 ^{a}	22 ± 6	32 ± 6 ^{f}
P_aO_2/F_iO_2, torr	243 ± 66	228 ± 88	255 ± 74	162 ± 67^{d}	351 ± 117	261 ± 112
P_aCO_2, torr	34 (30±41)	36 (32±51)	33 (30±40)	43 (41±46)	39 (36±42)	39 (33±43)

V_T=tidal volume; PEEP=positive end-expiratory pressure; RR=respiratory rate; F_IO_2=inspired O_2 fraction; CO=cardiac output; MAP=mean arterial pressure; MPAP=mean pulmonary arterial pressure; P_aO_2=arterial O_2 pressure; P_aCO_2=arterial CO_2 pressure. Data are shown as mean ± standard deviation if normally distributed, or median (25^{th}–75^{th} percentile) otherwise. Groups were compared using ANOVA with Tukey-Kramer post-hoc tests for normally distributed data, or Kruskall-Wallis with Bonferroni-corrected post-hoc tests otherwise, Time points were compared using paired t-tests.

a p<0.05 vs. Low-Strain LPS group.

b p<0.01 vs. Low-Strain LPS group.

c p<0.05 vs. High-Strain group.

d p<0.10 vs baseline.

e p<0.05 vs baseline.

f p<0.01 vs baseline.

Table 2

Regional Aeration and Regional and Global Tidal Strain

	High-Strain		High-Strain LPS		Low-Strain LPS	
Regional Variables:	**Baseline**	**End**	**Baseline**	**End**	**Baseline**	**End**
F_{EE}	0.45 ± 0.14 [a]	0.41 ± 0.14 [a]	0.50 ± 0.16 [a]	0.42 ± 0.17 [a]	0.69 ± 0.08	0.60 ± 0.12
ΔF_{EE}	−0.04 ± 0.08 [b]		−0.08 ± 0.10 [b]		−0.09 ± 0.10 [b]	
F_{EI}	0.62 ± 0.12 [a]	0.59 ± 0.14	0.67 ± 0.16	0.57 ± 0.21	0.74 ± 0.08	0.65 ± 0.12
ΔF_{EI}	−0.04 ± 0.05 [b]		−0.11 ± 0.14 [b]		−0.10 ± 0.10 [b]	
sVol	1.21 ± 0.62[a]	1.22 ± 0.51[a]	1.26 ± 0.44 [a]	1.05 ± 0.58[a]	0.33 ± 0.17	0.29 ± 0.18
ΔsVol	0.02 ± 0.49		−0.21 ± 0.51		−0.05 ± 0.11	
Global sVol	1.17 ± 0.49[a]	1.08 ± 0.23 [a]	1.06 ± 0.20 [a]	0.87 ± 0.31 [a]	0.31 ± 0.09	0.27 ± 0.13

F=fractional gas content; EE=end-expiration; EI=end-inspiration; Δ=change in parameter from baseline to end; sVol=tidal specific volume change (i.e., tidal strain); global sVol=sVol measured from whole-lung average F_{EE} and F_{EI}. Regional variables were compared between groups with a linear mixed-effects model including group as a fixed effect and random intercepts for each animal. Global sVol was compared between groups using ANOVA with Tukey-Kramer corrected post-hoc tests.

[a] $p<0.01$ vs. Low-Strain LPS group.

[b] $p<0.01$ for the hypothesis that the variable equals 0.